JOURNAL OF GEOPHYSICAL RESEARCH: ATMOSPHERES, VOL. 118, 1090–1099, doi:10.1029/2012JD018465, 2013

Variability of extratropical ozone stratosphere–troposphere exchange using microwave limb sounder observations

Mark A. Olsen,[1,2] Anne R. Douglass,[2] and Trevor B. Kaplan[3]

Received 10 July 2012; revised 4 November 2012; accepted 25 November 2012; published 31 January 2013.

[1] The extratropical stratosphere–troposphere exchange (STE) of ozone from 2005 to 2010 is estimated by combining Microwave Limb Sounder ozone observations and MERRA reanalysis meteorological fields in an established direct diagnostic framework. The multiyear mean ozone STE is 275 Tg yr^{-1} and 214 Tg yr^{-1} in the Northern and Southern Hemispheres, respectively. The year-to-year variability is greater in the Northern Hemisphere, where the difference between the highest and the lowest annual flux is 15% of the multiyear mean compared with 6% in the Southern Hemisphere. Variability of lower stratospheric ozone and variability of the net mass flux both contribute to interannual variability in the Northern Hemisphere ozone flux. The flux across the extratropical 380 K surface determines the amount of flux across the extratropical tropopause, and the greatest seasonal variability of the 380 K ozone flux occurs in the late winter/early spring, around the time of greatest flux. Both the mass flux and the ozone mixing ratios on the 380 K surface show recurring spatial patterns, but interannual variability of these quantities and their alignment contribute to the ozone flux variability. The spatial and temporal variability are not well represented when zonal and/or monthly mean fields are used to calculate the ozone STE, although this results in a small high bias of the seasonal amplitude and annual magnitude. If the climatological variability over these 6 years is representative, the estimated number of years required to detect a $2-3\%$ $decade^{-1}$ trend in ozone STE using this diagnostic is $35-39$ years.

Citation: Olsen, M. A., A. R. Douglass, and T. B. Kaplan (2013), Variability of extratropical ozone stratosphere–troposphere exchange using microwave limb sounder observations, *J. Geophys. Res. Atmos.*, *118*, 1090–1099, doi:10.1029/2012JD018465.

1. Introduction

[2] The magnitude and variability of upper tropospheric and lower stratospheric (UTLS) ozone and the stratosphere troposphere exchange (STE) of ozone are important to understanding the atmosphere's chemistry and climate. The flux of ozone from the stratosphere is important to the oxidizing capability of the troposphere [*Levy*, 1971]. Ozone and other greenhouse gases in the UTLS contribute to the radiative balance of the atmosphere [e.g., *Haywood et al*., 1998]. The ultraviolet (UV) index, a measure of exposure to potentially damaging solar UV radiation, is proportional to the total column ozone [*Madronich*, 2007]. Because the total column is computed as a mass-density-weighted vertical integral, the UTLS ozone accounts for ~15–50% of the column [e.g., *Wellemeyer et al*., 1997] and hence greatly impacts the UV index.

[3] The amount of ozone in the extratropical lowermost stratosphere between the tropopause and the 380 K potential temperature surface is controlled predominantly by transport of ozone-rich air from higher altitudes and quasihorizontal mixing of ozone-poor air from lower latitudes. Because the chemical lifetime of ozone in this region is much greater than the transport time scales, the ozone will ultimately pass into the troposphere through mixing or the downwelling branch of the Brewer-Dobson circulation [*Brewer*, 1949; *Dobson*, 1956].

[4] The STE of ozone cannot be measured explicitly, and many diagnostic methods have been used to estimate the net global or hemispheric STE from model simulations and observations. These methods range from direct calculations primarily using simulated quantities to indirect methods that use derived fields or empirical relationships. Direct methods have been used with model output where the vertical profiles of ozone are well resolved in the UTLS and are located on a sufficiently dense regular grid. For instance, *Clark et al*. [2007] use a variation of a diagnostic [*Wei*, 1987] that employs the vertical velocity, tropopause information, and ozone from a chemistry transport model (CTM) constrained by MOZAIC aircraft observations of ozone [*Marenco et al*., 1998]. As *Wirth and Egger* [1999] demonstrate, this diagnostic approach has large uncertainties, insofar as the

[1]Goddard Earth Sciences Technology and Research, Morgan State University, Baltimore, Maryland, USA.
[2]NASA Goddard Space Flight Center, Greenbelt, Maryland, USA.
[3]Science Systems and Applications, Inc., Greenbelt, Maryland Now at INNOVIM, Greenbelt, Maryland, USA.

Corresponding author: Mark A. Olsen, NASA Goddard Space Flight Center, Mailstop 614, Greenbelt, MD 20771, USA. (mark.a.olsen@nasa.gov)

2169-897X/13/2012JD018465

estimates are the small residual obtained when combining large terms. *Olsen et al*. [2004] compared the net STE of mass and ozone using a mass continuity diagnostic adapted from *Appenzeller et al*. [1996] that convolved the mass flux with CTM ozone output. *Hsu et al*. [2005] use a mass continuity approach at the model grid scale to evaluate the ozone STE in a CTM simulation.

[5] Estimates of STE using observations of ozone have been made with empirical diagnostic methods because global observational data sets of ozone vertical profiles prior to the launch of the Aura satellite in 2004 are relatively sparse and/or fail to measure the profile in the UTLS. These observational studies give best estimates of the global STE of ozone between 450 and 550 Tg yr^{-1}. *Murphy and Fahey* [1994] and *Olsen et al*. [2001] used correlative measures of nitrous oxide and ozone to estimate the flux of ozone to the troposphere. *Gettelman et al*. [1997] directly calculated the flux of ozone across the 50 hPa level using monthly zonal mean fields of UARS-observed ozone and residual vertical velocities derived from analyses. An empirical box model was then used to estimate the cross-tropopause flux. *Olsen et al*. [2003] estimated the net midlatitude ozone STE by using trajectories combined with the correlation of total column ozone from the Earth Probe Total Ozone Mapping Spectrometer (EP-TOMS) and column potential vorticity.

[6] Climate models predict an increasing trend in the Brewer-Dobson circulation over the next century. *Butchart et al*. [2006] examine multiple models and simulations and show that all models predict an increase in the tropical upwelling, with a multimodel mean trend of 11 kt s^{-1} yr^{-1} (about 2% per decade) and a range in the predicted trend of $0.1 - 17.8$ kt s^{-1} yr^{-1}. *Oman et al*. [2009] show that the large range in the predicted trends can be attributed to the varying sea surface temperature boundary conditions used by the models. An increase in ozone STE could occur from both an increase in the Brewer-Dobson circulation and decreases in ozone-depleting substances. *Hegglin and Shepherd* [2009] demonstrate a predicted 1.8% per decade trend in global ozone STE spanning $1965 - 2095$ and 2.6% per decade trend from 2000 to 2035 in a Chemistry Climate Model simulation.

[7] The current magnitude and variability of ozone STE must be known in order to understand the spatial and temporal measurement requirements needed to detect, quantify, and attribute a trend in STE. *Hsu and Prather* [2009] examine CTM simulated variability of ozone STE and the impact on tropospheric ozone. They find greater interannual ozone STE variability in the Sothern Hemisphere (SH), with the phase of the quasibiennial oscillation (QBO) causing 20% and 45% of the variance in the Northern Hemisphere (NH) and SH, respectively. However, the year-to-year variability of ozone STE derived from observations of ozone rather than from simulated ozone fields has not been investigated.

[8] In this study, we use Aura MLS ozone data within an established direct diagnostic framework to evaluate STE magnitude and variability over 6 complete years from 2005 through 2010. As noted above, several studies have used averaged fields in estimating the ozone flux. In the present study, we also show that the impact of using monthly and/or zonally averaged ozone fields is likely negligible for long time scale studies, such as trend analysis, but should be considered over shorter time scales. In the next section, we describe the data and analyses and give details on the STE diagnostic used in this study. The interannual and seasonal variability of the ozone and mass STE are presented in section 3 along with the analysis of the impact of using averaged fields. We follow with a summary and discussion of the results in the final section.

2. Data and Method

2.1. Data and Analyses

[9] Ozone mixing ratios from the Aura MLS v3.3 level 2 retrievals are used in the present study. The data are screened as recommended by *Livesey et al*. [2011]. The vertical resolution of the MLS v3.3 data is ~2.5 km in the lower stratosphere and contains usable data down to 261 hPa. Measurements are reported along track at ~200 km resolution. The longitudinal spacing between orbits is about 25° at middle latitudes. We increase the effective horizontal resolution of the MLS data by using the trajectory mapping technique of *Schoeberl et al*. [2007]. This method uses 2-day forward and backward 3-D trajectories to map MLS profile data to a regular $1.25° \times 1°$ longitude – latitude grid. Currently, 6 complete years from 2005 through 2010 have been processed using this technique, so our analysis is limited to this time frame. In the case of missing data (generally 2 to 14 nonsequential days per year), we interpolate the ozone data linearly in time.

[10] Both the trajectories and the mass fluxes are calculated by using analyses from Modern Era Retrospective-Analyses for Research and Applications (MERRA) produced by the NASA Global Modeling and Analysis Office [*Rienecker et al*., 2011]. The MERRA output is produced using the GEOS-5 Assimilation System, in which the underlying atmospheric model is the GEOS-5 General Circulation Model (GCM) [*Rienecker et al*., 2008]. The analysis fields used for the trajectory mapping and mass flux calculations are saved on a $1.25° \times 1.25°$ grid (degraded from the native model resolution of $0.67° \times 0.5°$) with a vertical spacing of $\sim 2 - 2.5$ km in the lower stratospheric region of interest.

2.2. STE Diagnostic

[11] *Appenzeller et al*. [1996] used a mass conservation approach to diagnose extratropical mass STE as the sum of the flow into the lowermost stratosphere and the time rate of change of mass in that region. The diagnostic was adapted by *Schoeberl* [2004] to compute the mass flux using heating rates on the 380 K potential temperature surface upper boundary rather than the residual vertical velocities on the 100 hPa surface. *Olsen et al*. [2004] first used this diagnostic approach to estimate ozone STE with the output from a CTM. We follow this method where the net extratropical tropopause flux in each hemisphere is determined from the rate of change in lowermost stratospheric mass (M, between the tropopause and the 380 K surface) and the diabatic flux across the 380 K surface (F_{380K}),

$$F_{trop} = \frac{dM}{dt} + F_{380K}. \quad (1)$$

[12] We use daily average analyses of heating rates to compute the 380 K mass flux. We determine the ozone flux by convolving the computed mass flux with the MLS ozone mixing ratios at every grid point. We consider the flux only

where the mass between the tropopause and 380 K surface exceeds 30 g cm^{-2} [*Schoeberl*, 2004; *Olsen et al.*, 2004]. This definition dividing the tropics and extratropics approximates the zero zonal mean heating rate line on the 380 K surface. Thus, the width of the tropics is more reasonable compared with diagnostic approaches that consider the flux poleward of the intersection of the dynamical (based on potential vorticity) tropopause and the upper boundary.

[13] In the present work, we focus on the 380 K ozone flux rather than the tropopause flux as determined by the mass balance of equation 1. The extratropical tropopause frequently lies below 261 hPa, the lowest altitude of valid MLS data. Therefore, the time rate of change of ozone mass in the lowermost stratosphere cannot be accurately calculated. The magnitude of ozone flux across the tropopause for any given year may be slightly different from the 380 K ozone flux because the annually integrated time rate of change of ozone mass is not necessarily zero. However, the longer-term mean and the year-to-year variability of the ozone STE are still well represented. We have similarly calculated the 380 K and tropopause flux using a Global Modeling Initiative CTM [*Strahan et al.*, 2007] simulation driven by MERRA analyses over the same time period. With the assumption that the lowermost stratospheric chemical loss of ozone is negligible [i.e., *Olsen et al.*, 2004], the simulated 6 year mean annual tropopause flux of ozone is less than 1% different from the mean 380 K flux. For the remainder of this article, any reference to simply the mass or ozone flux will refer specifically to the flux across the 380 K surface unless the tropopause is explicitly stated.

3. Results

[14] Conceptually, the ozone flux is the area-integrated product of the mass flux and the ozone mixing ratio at the flux surface. We consider these factors in the NH by examining 6 year monthly mean values during February (Figure 1). As we show below in this section, this month is near the seasonal maxima of both ozone flux and year-to-year variability. Figure 1a shows the February mean ozone distribution on the 380 K surface. The ozone mixing ratios generally increase with latitude but become much less zonally symmetric poleward of ~40°N. Zonal maxima occur near 80°W and 130°E at about 60° N. The flux of mass across 380 K is greatest at midlatitudes (Figure 1b), in contrast to the ozone distribution. Local maxima are seen around 40°N in a zonal wave 4 pattern near 5°W, 90°W, 160°E, and 70°E.

[15] Figure 1c shows the February mean ozone flux calculated from the daily values of the ozone flux. Similar to the mass flux, a large fraction of the net ozone flux occurs at midlatitudes, although the ozone flux maxima occur farther poleward as a result of the poleward increasing ozone distribution. The pattern of ozone flux is notably dissimilar to the ozone distribution. In particular, the two greatest ozone flux maxima occur near 90°W and 170°E, whereas the contours of ozone mixing ratio tend to be displaced off the pole over the Asian continent. These results illustrate that the short-time-scale ozone flux is sensitive to the zonal asymmetries of the mass flux and ozone distribution and the spatial orientation of the flux and distribution.

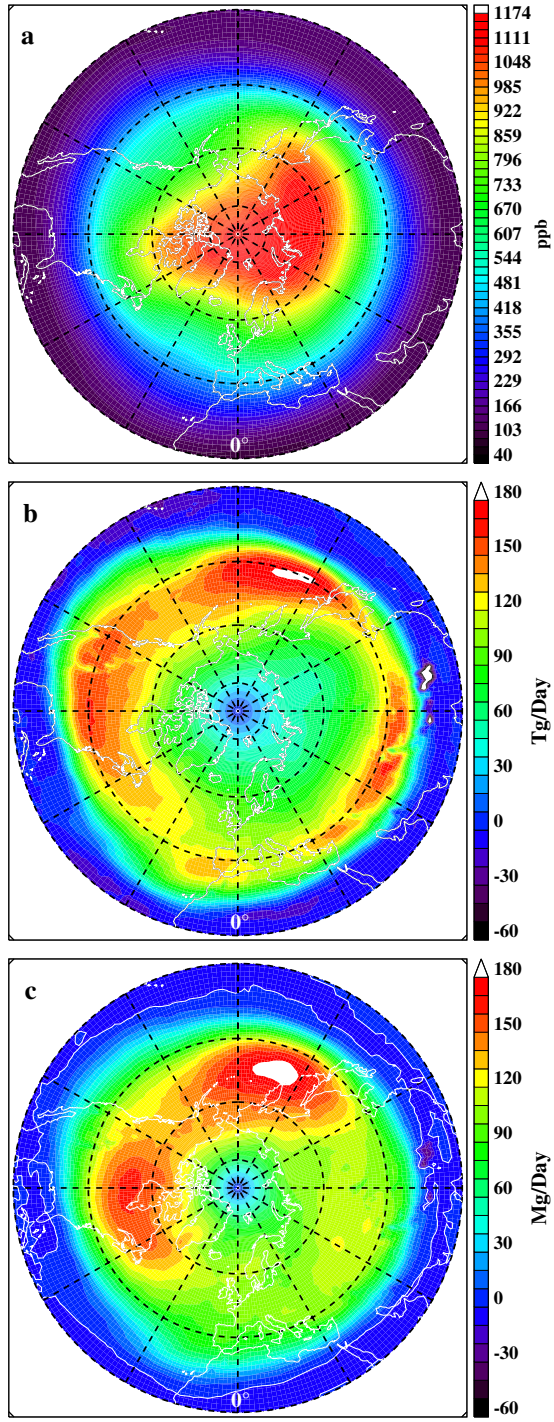

Figure 1. February average daily (a) ozone distribution on the 380 K potential temperature surface, (b) net mass flux across the 380 K surface, and (c) net ozone flux across the 380 K surface. The Northern Hemisphere is shown beginning at 20°N, with latitude lines every 20°. Positive flux values correspond to downward flux.

[16] The annual magnitudes of the extratropical ozone flux for 2005 to 2010 are shown as solid lines in Figure 2. The 6 year net mean NH and SH extratropical flux is 489 Tg yr^{-1}, with 275 Tg yr^{-1} (56%) in the NH and 214 Tg yr^{-1} (44%) in the SH. These values are similar to results of

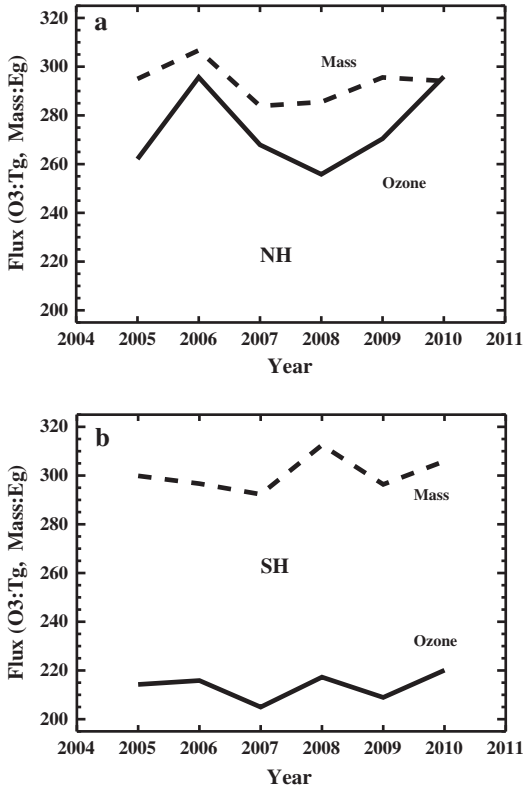

Figure 2. The annual ozone (solid lines) and mass (dashed lines) flux across the extratropical 380 K surface in the (a) NH and (b) SH for the years 2005–2010.

previous studies that use ozone observations with empirically based approaches to determine the ozone STE. *Gettelman et al*. [1997] used a similar mass flux diagnostic to calculate the ozone flux at 50 hPa and empirically extrapolate the results to 100 hPa as an estimate of the STE. They arrived at a best estimate net NH and SH extratropical flux of 510 Tg yr^{-1}, with 57% in the NH. *Olsen et al*. [2001] estimated that the net NH and SH extratropical flux of ozone is 550 ± 140 Tg yr^{-1}, derived from correlations of NO_y and N_2O. *Olsen et al*. [2003] used the correlation of column ozone and column PV to estimate the midlatitude (between 30° and 60° latitude) tropopause flux of ozone to be 260 Tg yr^{-1} in the NH and 210 Tg yr^{-1} in the SH.

[17] The annual values of ozone flux in Figure 2 show that the year-to-year variability is greater in the NH than in the SH. The difference between the highest and lowest annual flux is about 15% of the multiyear mean in the NH compared with about 6% of the mean in the SH. This contrasts with the results of a CTM simulation by *Hsu and Prather* [2009], who found that the interannual variability is greater in the SH. The mass flux variability is similar in each hemisphere in the present study, with the maximum – minimum difference being 8% of the mean in the NH and 7% of the mean in the SH (Figure 2). Thus, the greater variability of ozone STE in the NH must be due primarily to greater variability of ozone in the NH lower stratosphere. The zonal asymmetries at 380 K discussed relative to Figure 1 and the annual flux values in Figure 2 demonstrate that there is not a simple relationship between the ozone flux and the mass flux.

[18] The mean annual cycle of ozone and mass flux and yearly anomalies are shown in Figure 3. We note that the annual cycles agree well with the model results of *Olsen et al*. [2004], although the NH minimum ozone flux occurs about 1 month sooner than in the simulation. The NH mass flux minimum occurs at about the same time in both the present results and the *Olsen et al*. simulation. Therefore, the summertime minimum of the prior study's simulated ozone on the 380 K surface occurs later than observed by MLS.

[19] The greatest year-to-year variability of the NH ozone flux occurs in the late winter/early spring, from the beginning of the year to about the end of March. This coincides with the timing of the maximum flux and the period just after the maximum. The interannual variability of the ozone flux is least in the summer and early fall, following the summertime flux minimum. Figure 3 shows absolute differences from the 6 year mean rather than percentage differences. The largest differences from the 2005 – 1010 mean occur in winter and spring, but the percentage differences from the mean are nearly constant throughout the year (not shown). However, the greatest contribution to the differences in the annual flux comes from the large variability of the absolute anomalies in the winter and spring.

[20] *Olsen et al*. [2004] estimated a residence time scale of ozone in the lowermost stratosphere on the order of 100 days. They show that, consistent with this time scale of transport from 380 K to the tropopause, the ozone flux across the tropopause is expected to be greatest in the spring and early summer. In the present study, the net January to March 380 K ozone flux is greatest in 2006. This suggests that the spring/summer tropopause ozone flux should be greatest in 2006. Although the annual net 380 K flux is the same in 2006 and 2010, the seasonality of the flux varies. The flux during the beginning of the year in 2010 was less than that in 2006, but the 2010 flux was larger during the latter half of the year. In fact, the 2010 flux remains greater than the multiyear mean throughout the entire year.

[21] In the SH, the greatest variability in the ozone flux occurs in the late fall/early winter (Figure 3). This is at and before the maximum flux, contrasting with the NH. The variability in the SH during the fall to spring is generally less than that in the NH during these seasons.

[22] We next consider the mean cycles of mass flux and yearly anomalies shown in Figure 3. The seasonal variability of the mass flux in the SH is similar in magnitude and seasonality to the NH. The mass and ozone flux cycles are nearly in phase in the NH. In the SH, the mass flux maximum precedes the ozone flux maximum by about 1 month. In both hemispheres, the mass flux summer minimum is not as broad as the ozone flux minimum. The mass flux tends to increase more rapidly than the ozone flux for several months following the minimum. At this time, the ozone mixing ratios on the 380 K surface are near their annual minimum (not shown). The seasonal cycles shown here are generally consistent with the CTM results of *Olsen et al*. [2004]. However, in that simulation, the phase of the NH mass flux led the ozone flux by about 1 month, similar to the SH. This contrast again illustrates that the previous study's simulated 380 K ozone must differ from the observed ozone, resulting in a phase shift of the ozone flux.

[23] The differences between mass and ozone flux variability seen in Figure 3 emphasizes that the ozone flux

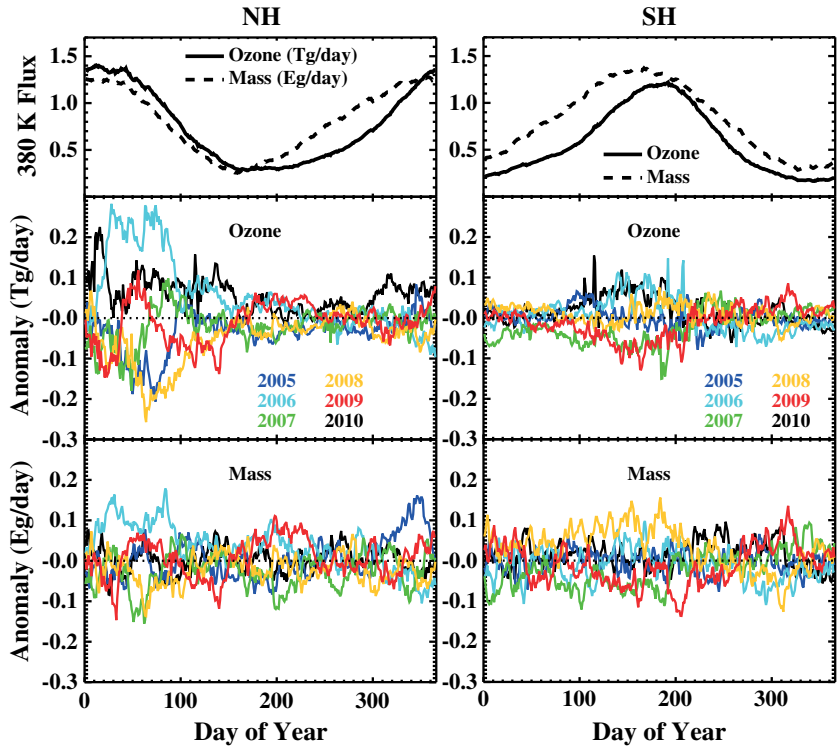

Figure 3. Annual cycles of the net extratropical 380 K ozone and mass fluxes in the NH and SH. Top panels show the 6-year mean, and the bottom panels are the ozone and mass flux anomalies for each year with respect to the mean.

variability must be significantly influenced by other factors, such as the amount of quasihorizontal transport in the lower stratosphere. The NH year-to-year variability in the mass flux over seasonal time scales is greatest in the winter and early spring, similar to that of the ozone flux. However, this winter/spring mass flux variability is not much greater than the variability in the summer and fall seasons. Both the interannual and interseasonal variance of the mass flux is not as great as that of the ozone flux. Although the seasonal cycles of mass and ozone flux are nearly in phase and exhibit similar patterns of year-to-year seasonal variability, the relative magnitude of the mass flux for any particular season and year does not necessarily indicate the relative magnitude of the ozone flux. For example, the mass flux is greatest in the winter/spring of 2006 and, likewise, the ozone flux is also greatest at this time, implying that the greater mass flux has a primary role in this instance of increased ozone flux. However, during the same period in 2010, the mass flux remains close to the multiyear mean, whereas the magnitude of the ozone flux is second only to 2006. The mean mixing ratio of ozone in the mass of air transported across the 380 K surface is relatively large at this time in 2010 compared with other years.

[24] The NH February mean 380 K ozone mixing ratios are shown for each year in Figure 4. There are considerable year-to-year differences in both the magnitude and the spatial distribution of ozone. However, the distribution patterns in 2005, 2007, and 2008 are similar and clearly dominate the multiyear average shown in Figure 1a. In these years, the maximum hemispheric ozone value is greater, and the distributions are more zonally symmetric over the polar regions compared with the other years. These are the years with the least amount of ozone flux in February (Figure 3). In the other 3 years, the maximum ozone values are not as large, and the ozone distributions are less zonally symmetric with the pattern "pushed off the pole," primarily over western Asia and the eastern Pacific, indicating greater wave activity. Although the hemispheric maximum ozone values are actually less than those in 2005, 2007, and 2008, this increased wave forcing contributes to an increased ozone flux in two intertwined ways. First, the net mass flux is increased through greater stratospheric meridional and downward transport described by the "downward control" principle [*Haynes et al.*, 1991]. Second, the equatorward transport displaces the ozone-rich polar air toward the midlatitudes where the descending mass flux is greatest.

[25] The year-to-year spatial pattern of mass flux maxima on the 380 K surface does not deviate much from the multiyear mean pattern shown in Figure 1b (year-to-year values not shown). However, the relative magnitudes of the maxima vary considerably. The February mean ozone flux obtained by convolving the daily mass flux and ozone distribution is shown for each year in Figure 5. As in the multiyear mean (Figure 1c), most of the ozone flux occurs at midlatitudes every year, regardless of the various ozone distributions on the 380 K surface. Like the 380 K ozone distribution, the spatial patterns of the ozone flux in 2005, 2007, and 2008 are similar. These years dominate the multiyear mean, although the 6 years of observations examined here are insufficient to generalize this pattern as climatology.

[26] The two midlatitude ozone flux maxima seen in the multiyear mean over the western Pacific around 160 – 180°E

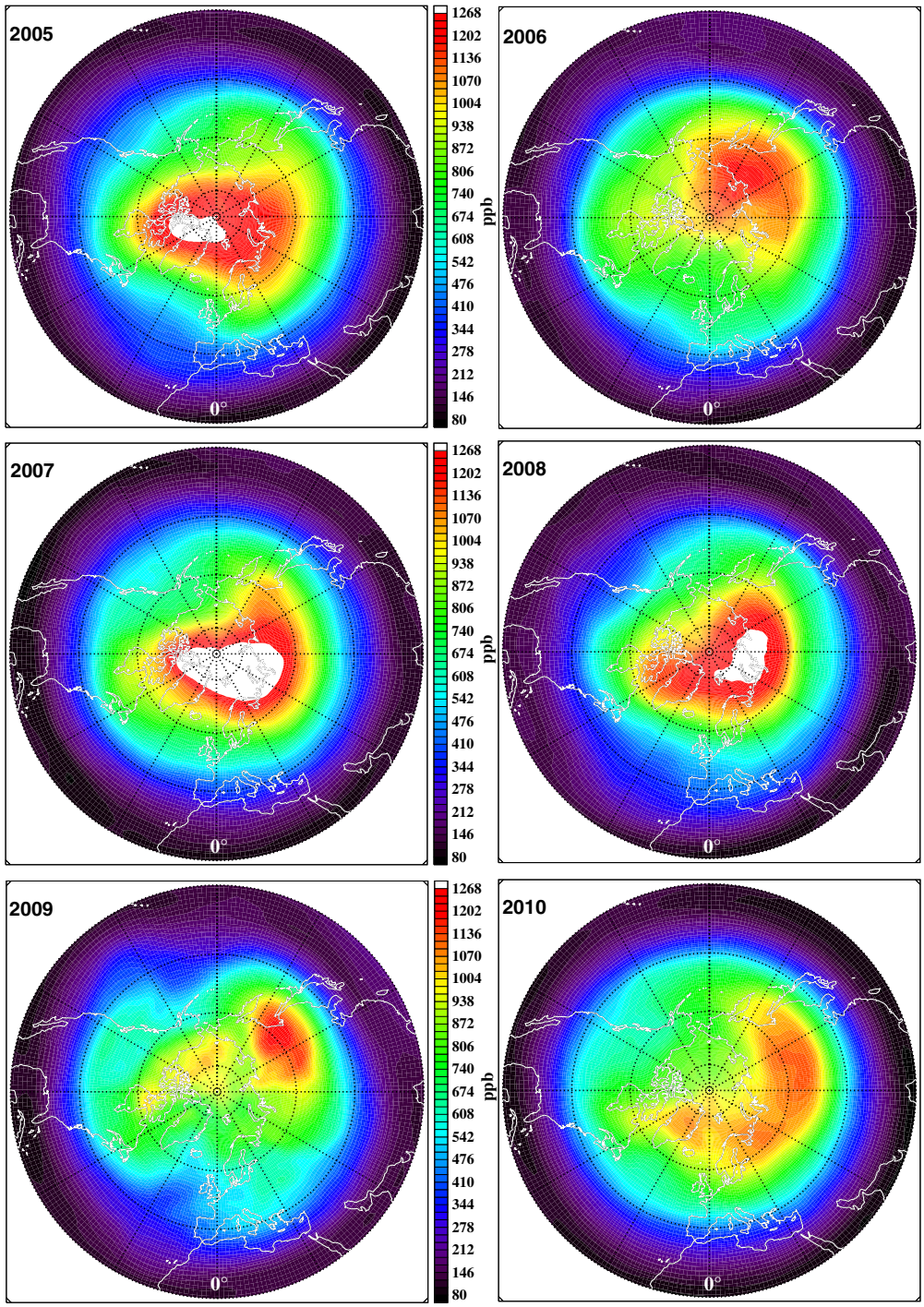

Figure 4. February mean ozone distributions on the 380 K surface for years 2005–2010. The Northern Hemisphere is shown beginning at 20°N, with latitude lines every 20°.

and over North America near 90°W are relatively consistent preferred regions of ozone flux. The ozone flux in the western Pacific region is usually greatest, although the flux in these regions is highly variable.

[27] The spatial patterns of ozone flux in all 6 years have some similar features. However, the 2 years of greatest annual and February ozone flux, 2006 and 2010, exhibit spatial patterns that are distinctly different. In 2006, the maximum over North America is significantly greater than any other year, and there is a significant maximum over eastern Europe. The western Pacific maximum is shifted much more eastward in 2010 compared with all other years. The North American maximum is also greatly reduced in magnitude, with a significant increase in flux over the Atlantic in 2010. It is likely that these differences in 2006 and 2010, as well as the greater flux over Europe in 2009, are a result of major stratospheric sudden warming events that occurred in late January of those years.

[28] The seasonal variability and zonal asymmetry of the ozone distribution and fluxes presented here suggest that

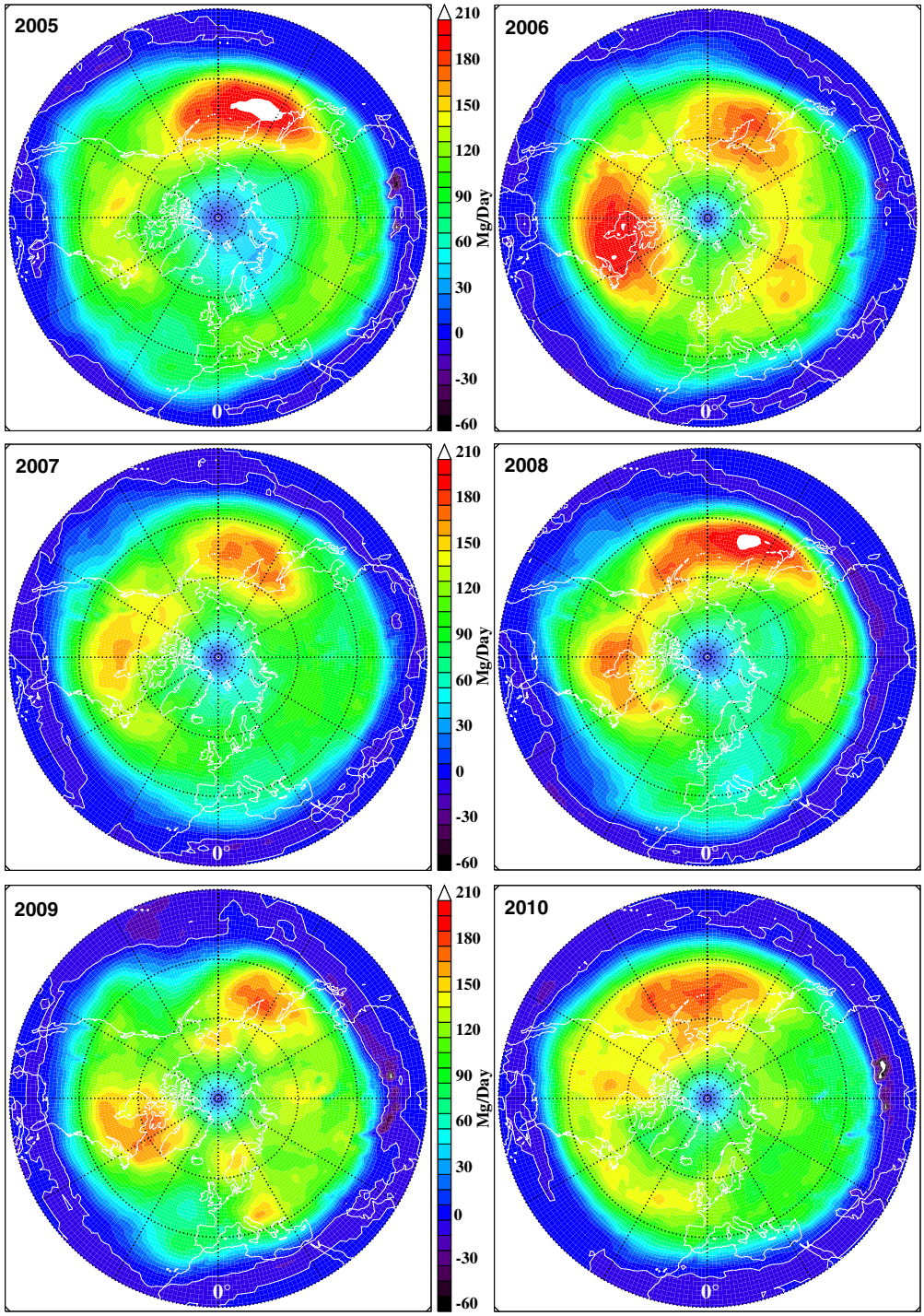

Figure 5. February mean 380 K ozone flux for years 2005–2010. The Northern Hemisphere is shown beginning at 20°N, with latitude lines every 20°. Positive flux values correspond to downward flux, where the white contour line denotes zero net flux.

the spatial and temporal resolution of the ozone and meteorological fields used in calculating the STE is important to consider. The resolution of these fields used in studies that estimate ozone flux can vary significantly. For example, previous studies using a form of the mass balance diagnostic of ozone STE have employed various spatial and temporal resolution ozone fields. *Olsen et al*. [2004] applied 3-D, daily CTM ozone fields to calculate the STE. *Gettelman et al*. [1997] and *Hegglin and Shepherd* [2009] used zonal, monthly mean ozone from observations and model output, respectively. Here, we investigate possible systematic differences from using averaged fields in order to provide context for comparing the results of various studies. We compare the STE estimates computed using daily 3-D fields of the current study with estimates calculated using the same diagnostic with zonal and/or monthly mean fields.

[29] Estimates of STE have been calculated using ozone and mass flux fields that have been averaged in three ways: (1) using monthly mean fields, (2) using zonal mean fields, and (3) using zonal monthly mean fields. The mass flux is still calculated with the daily 3-D fields and before averaging. In addition, we quantify the information gained by increasing the effective horizontal resolution of the MLS data using the trajectory mapping technique in this study. For this, we use daily 3-D fields of ozone by linearly interpolating each day's MLS measurements to the $1.25° \times 1°$ longitude – latitude grid rather than using the trajectory mapping technique.

[30] The results of the ozone flux calculated using the different fields are listed in Table 1. We show the multiyear mean February, August, and annual fluxes in the NH for each case. February and August are chosen as representative of periods with considerable and little interannual variability of the ozone flux, respectively.

[31] Systematic biases exist using the averaged fields, but the errors are small compared with uncertainties in the ozone data and meteorological analyses. The mean February fluxes are slightly overestimated in each case using mean fields in the computation of STE. The February flux estimate using the monthly mean fields are about 4% greater than that of the 3-D, daily-resolved fields. Likewise, the computations employing the zonal mean and the zonal, monthly mean fields are about 5% and 6% greater, respectively. The STE estimates using the mean fields are consistently overestimated in every year during all the winter/spring months (not shown), when the mass flux and ozone distributions are most variable and zonally asymmetric. The spatially and/or temporally averaged fields fail to capture this variability in a manner that results in a greater estimated flux.

[32] During August and other summer/fall months, the mass flux and ozone distributions are less variable and more zonally symmetric. The ozone flux computed using the averaged fields during these months is nearly equal (~1% less) to the 3-D, daily field estimate of flux. Consequently, the bias introduced by using the mean fields is seasonally dependent and results in a seasonal cycle magnitude that is too large.

[33] The calculated annual mean ozone flux is about the same with any zonal and/or monthly mean fields. Given the seasonal dependence of the relative differences, the annual values are only slightly overestimated, by a little over 2%, compared with the net flux of 275 Tg obtained using the fields without spatial and temporal averaging.

[34] The ozone flux estimated with the linear horizontal interpolated ozone data is less than 1% different from that calculated from the trajectory-mapped data over all months. Thus, a simple interpolation of the data obtained from the ~15 orbits per day by MLS is sufficient to characterize the spatial variability of the lower stratospheric ozone in the calculation of the ozone flux. Smaller scale features that are revealed by using trajectory mapping do not significantly contribute to the ozone flux estimate.

Table 1. Six-Year Mean NH Extratropical 380 K Ozone Flux

Fields Used	February Mean Ozone Flux (Tg day^{-1})	August Mean Ozone Flux (Tg day^{-1})	Annual Mean Ozone Flux (Tg)
3-D, daily mean	1.30	0.359	275
3-D, monthly mean	1.35	0.356	281
Zonal, daily mean	1.37	0.354	281
Zonal, monthly mean	1.38	0.355	282
Linear interpolated O_3	1.29	0.360	273

4. Discussion and Conclusions

[35] We have used an established direct STE diagnostic framework with observed ozone data from Aura MLS to examine the magnitude and variability of the ozone flux over 6 years. The mean annual ozone flux from 2005 to 2010 is estimated to be 275 Tg and 214 Tg in the NH and SH, respectively.

[36] The magnitude of the annual ozone flux is much more variable in the NH than in the SH. The difference between the maximum and minimum annual flux is about 15% of the mean in the NH and only about 6% in the SH. Most of this variability in the annual flux across the 380 K surface occurs in the late winter/early spring in the NH and late fall/early winter in the SH, near the time of maximum flux. However, the seasonal cycle of ozone flux across the 380 K surface remains relatively consistent. The temporal separation of the yearly extremes is about 1 month or less. The timing of maximum and minimum flux across the tropopause, rather than the 380 K surface, could be more variable from year to year. *Olsen et al*. [2004] show that the phase of the seasonal cycle of ozone flux across the tropopause is dominated by the seasonal transition of the mean extratropical tropopause height, similar to that of the mass flux demonstrated by *Appenzeller et al*. [1996]. Therefore, we expect the variability in the phase of the tropopause flux seasonal cycle to be small, similar to the phase variability of the 380 K flux.

[37] The mass flux and ozone flux across the 380 K surface are nearly in phase. However, as *Olsen et al*. [2004] demonstrated for the tropopause, we show that there is not a direct or simple proportional relationship between the mass flux and ozone flux at the 380 K surface. This emphasizes that the magnitude of ozone STE and the amount of ozone in the lower stratosphere are not due solely to the strength of the downwelling Brewer-Dobson circulation. Quasihorizontal transport from lower latitudes into the extratropics brings air with lower concentrations of ozone into the lower stratosphere. *Olsen et al*. [2010] show that the net meridional transport in the lower stratosphere can vary greatly from year to year. It is reasonable to expect that differences in the net quasihorizontal transport above the 380 K surface will contribute to the variability in the downward flux of ozone across the surface. In addition, the present work shows that spatial distributions of ozone at 380 K are not indicative of the net mass flux on this surface. During the short time period of this study, there were distinct, preferred patterns for both of these quantities. Deviations from these patterns and changes to the alignment of these fields with respect to each other can be a significant source of the ozone flux variability on seasonal time scales. These results are important to the interpretation of simulations from models that use a simplified stratospheric ozone scheme, such as tropospheric models that relax stratospheric ozone to climatology.

Although the mass flux variability may be well reproduced, the ozone flux variability will be underrepresented.

[38] Climate models predict an increase in the Brewer-Dobson circulation throughout the next century with the multimodel mean rate of about 2% per decade [*Butchart et al*., 2006]. *Hegglin and Shepherd* [2009] show an increase of the ozone STE in a chemistry climate model simulation between 2000 and 2035 of about 3.1% per decade and 2.0% per decade in the NH and SH, respectively. Their simulated global extratropical trend is about 2.6% per decade. These increases are due to both climate change and ozone recovery during this period.

[39] If the variability of the ozone flux for the 6 years examined here is representative of the longer term climatology, multidecadal observations will be needed to detect a significant increasing trend using the flux diagnostic of this study. We use the statistical model described by *Weatherhead et al*. [1998] to determine the number of years required to have a 90% probability of detecting a trend at the 95% confidence level, assuming that comparable ozone observations continue. The standard deviation and autocorrelation of the detrended and deseasonalized monthly mean ozone flux time series of this study are used, and we assume the simulated trends from 2000 to 2035 found by *Hegglin and Shepherd* [2009]. Table 2 shows the best estimates for the number of years required to detect the hemispheric and global trends and the associated ranges of uncertainty. Identifying trends in the NH and SH flux would require nearly the same number of years. The SH has less variability than the NH, but the assumed trend is also smaller in the SH. Using the estimate of global extratropical flux slightly reduces the estimated years required because the variance of the global time series is slightly less than that of either hemisphere alone. However, the considerable overlap of the large ranges of uncertainty shows that this difference is not significant. The large ranges of uncertainty are due to large autocorrelations of the monthly time series.

[40] Finally, the use of temporally or spatially averaged fields within this diagnostic framework introduces a small bias in the estimated ozone flux resulting from the asymmetry of the ozone distribution and mass flux fields. The estimated fluxes are about 6% greater using both monthly and zonally averaged fields compared with the flux calculation using daily latitude – longitude fields during months of greatest flux. This high bias is reduced to about 2% over annual time scales. The magnitude of the seasonal cycle of ozone flux is also slightly exaggerated because of the seasonal dependence of the bias. The zonal monthly mean fields likely are adequate to use in long-time-scale studies, such as trend analysis. The use of nonaveraged fields to calculate the flux is appropriate over shorter time scales or when the best estimate is necessary. In addition, this assessment provides context for comparing estimates made using different average fields.

Table 2. Estimated Number of Years To Detect a Significant Trend in 380 K Ozone Flux[1]

Extratropical Region	Assumed Trend (% per Decade)	Best Estimate (Years)	Range (Years)
Northern Hemisphere	3.1	38	26–55
Southern Hemisphere	2.0	39	26–58
Global	2.6	35	23–52

[1]Results are rounded up to the nearest whole year. Assumed trends are based on the results of *Hegglin and Shepherd* [2009].

[41] **Acknowledgments.** The authors thank the anonymous referees that provided constructive comments to improve the manuscript. This work was supported by NASA's ACMAP program.

References

Appenzeller, C., J. R. Holton, and K. H. Rosenlof (1996), Seasonal variation of mass transport across the tropopause, *J. Geophys. Res.*, *101*, 15071–15078.

Brewer, A. M. (1949), Evidence for a world circulation provided by the measurements of helium and water vapor distribution in the stratosphere, *Q. J. R. Meteorol. Soc.*, *75*, 351–363.

Butchart, N., et al. (2006), Simulations of anthropogenic change in the strength of the Brewer-Dobson circulation, *Clim. Dyn. 27*, 727–741.

Clark, H. L., M.-L. Cathala, H. Teyssessdre, J.-P. Cammas, and V.-H. Peuch (2007), Cross-tropopause fluxes of ozone using assimilation of MOZAIC observations in a global CTM, *Tellus*, *59B*, 39–49.

Dobson, G. M. B. (1956), Origin and distribution of polyatomic molecules in the atmosphere, *Proc. R. Soc. Lond. Ser. A*, *236*, 187–193.

Gettelman, A., J. R. Holton, and K. H. Rosenlof (1997), Mass fluxes of O3, CH4, N2O and CF2Cl2 in the lower stratosphere calculated from observational data, *J. Geophys. Res.*, *102*, 19149–19159.

Haynes, P. H., M. E. McIntyre, T. G. Sheperd, C. J. Marks, and K. P. Shine (1991), On the "downward control" principle of extratropical circulations by eddy-induced mean zonal forces, *J. Atmos. Sci.*, *48*, 651–678.

Haywood, J. M., M. D. Schwartzkopf, and V. Ramaswamy (1998), Estimates of radiative forcing due to modeled increases in tropospheric ozone, *J. Geophys. Res.*, *103*, 16,999–17,007.

Hegglin, M. I., and T. G. Shepherd (2009), Large climate-induced changes in ultraviolet index and stratosphere-to-troposphere ozone flux, *Nat. Geosci.*, *2*, 687–691.

Hsu, J., and M. J. Prather (2009), Stratospheric variability and tropospheric ozone, *J. Geophys. Res.*, *114*, D06102, doi:10.1029/2008JD010942.

Hsu, J., M. J. Prather, and O. Wild (2005), Diagnosing the stratosphere-to-troposphere flux of ozone in a chemistry transport model, *J. Geophys. Res.*, *110*, D19305, doi:10.1029/2005JD006045.

Levy, H., II (1971), Normal atmosphere: Large radical and formaldehyde concentrations predicted, *Science*, *173*, 141–143.

Livesey *et al*. (2011), EOS MLS Version 3.3 Level 2 data quality and description document, Technical report, Jet Propulsion Laboratory, D-33509. Available at http://mls.jpl.nasa.gov.

Madronich, S. (2007), Analytic formula for the clear-sky UV index, *Photochem. Photobiol.*, *83*, 1537–1538.

Marenco, A., V. Thouret, P. Nedelec, H. G. Smit, M. Helten, D. Kley, F. Karcher, P. Simon, K. Law, J. Pyle, G. Poschmann, R. V. Wrede, C. Hume, and T. Cook (1998), Measurement of ozone and water vapour by Airbus in-service aircraft: the MOZAIC airborne program, an overview, *J. Geophys. Res.*, *103*, 25631–25242.

Murphy, D. M., and D. W. Fahey (1994), An estimate of the flux of stratospheric reactive nitrogen and ozone into the troposphere, *J. Geophys. Res.*, *99*, 5325–5332.

Olsen, M. A., A. R. Douglass, and M. R. Schoeberl (2003), A comparison of Northern and Southern Hemisphere cross-tropopause ozone flux, *Geophys. Res. Lett.*, *30*(7), 1412, doi:10.1029/2002GL016538.

Olsen, M. A., M. R. Schoeberl, and A. R. Douglass (2004), Stratosphere troposphere exchange of mass and ozone, *J. Geophys. Res. 109*, D24114, doi:10.1029/2004JD005186.

Olsen, M. A., A. R. Douglass, M. R. Schoeberl, J. M. Rodriguez, and Y. Yoshida (2010), Interannual variability of ozone in the winter lower stratosphere and the relationship to lamina and irreversible transport, *J. Geophys. Res.*, *115*, D15305, doi:10.1029/2009JD013004.

Olsen, S.C., C.A. McLinden, and M.J. Prather (2001), Stratospheric N2O-NOy system: Testing uncertainties in a three-dimensional framework, *J. Geophys. Res.*, *106*(B7), 28771–28784, doi:10.1029/2000JB900453.

Oman, L., D. W. Waugh, S. Pawson, R. S. Stolarski, and P. A. Newman (2009), On the influence of anthropogenic forcings on changes in the stratospheric mean age, *J. Geophys. Res.*, *114*, D03105, doi:10.1029/2008JD010378.

Rienecker, M. M., M. J. Suarez, R. Todling, J. Bacmeister, L. Takacs, H.-C. Liu, W. Gu, M. Sienkiewicz, R.D. Koster, R. Gelaro, I. Stajner,

and E. Nielsen (2008), The GEOS-5 Data Assimilation System—Documentation of Versions 5.0.1, 5.1.0, and 5.2.0. Technical Report Series on Global Modeling and Data Assimilation 104606, v27.

Rienecker, M. M., M. J. Suarez, R. Gelaro, R. Todling, J. Bacmeister, E. Liu, M. G. Bosilovich, S. D. Schubert, L. Takacs, G.-K. Kim, S. Bloom, J. Chen, D. Collins, A. Conaty, A. da Silva, et al. (2011), MERRA—NASA's Modern-Era Retrospective Analysis for Research and Applications, *J. Clim.*, *24*, 3624–3648, doi:10.1175/JCLI-D-11-00015.1.

Schoeberl, M. R. (2004), Extratropical stratosphere-troposphere mass exchange, *J. Geophys. Res.*, *109*, D13303, doi:10.1029/2004JD004525.

Schoeberl, M. R., et al. (2007), A trajectory-based estimate of the tropospheric ozone column using the residual method, *J. Geophys. Res.*, *112* (D24), D24S49, doi:10.1029/2007JD008773.

Strahan, S. E., B. N. Duncan, and P. Hoor (2007), Observationally derived transport diagnostics for the lowermost stratosphere and their application to the GMI chemistry and transport model, *Atmos. Chem. Phys.*, *7*, 2435–244.

Weatherhead, E. C., et al. (1998), Factors affecting the detection of trends: Statistical considerations and applications to environmental data, *J. Geophys. Res.*, *103*(D14), 17149–17161.

Wei, M. Y. (1987), A new formulation of the exchange of mass and trace constituents between the stratosphere and troposphere, *J. Atmos. Sci.*, *44*, 3079–3086.

Wellemeyer, C. G., S. L. Taylor, C. J. Seftor, R. D. McPeters, and P. K. Bhartia (1997), A correction for total ozone mapping spectrometer profile shape errors at high latitude, *J. Geophys. Res.*, *102*(D7), 9029–9038, doi:10.1029/96JD03965.

Wirth, V., and J. Egger (1999), Diagnosing extratropical synoptic-scale stratosphere – troposphere exchange: A case study, *Q. J. R. Meteorol. Soc.*, *125*, 635–655.